Optical coatings for glazings

C. Granqvist

JOURNAL DE PHYSIQUE IV
Colloque C7, supplément au Journal de Physique III, Volume 3, novembre 1993

Optical coatings for glazings

C.G. GRANQVIST

Physics Department, Chalmers University of Technology and University of Gothenburg, Gothenburg, Sweden

ABSTRACT

This paper reviews the state of the art for optical coatings for glazings and gives a view to some developments that will be feasible in the near future. Emphasis is put on coatings for energy efficiency and solar energy applications, and key concepts such as spectral and angular selectivity, large-area chromogenics, and smart windows are introduced and discussed. Recent advances in electrochromic coatings are covered in some depth.

I. INTRODUCTION

Materials with tailor-made radiative properties are useful for harnessing the Sun's energy, for creating a new energy-efficient architecture, etc. The materials optimization must be done with consideration of the radiation that prevails naturally in our surroundings. This paper discusses this "natural" radiation, and uses its characteristic properties to devise coatings for various types energy-efficient buildings. Emphasis is put on large-area chromogenics, which enables "smart windows" to be realized. A particularly interesting alternative uses electrochromic thin films to regulate the throughput of radiant energy so that a desirable indoor temperature and a desirable level of illumination are maintained.

Section II below introduces spectra for thermal and solar radiation, for atmospheric absorptance, and for visible and photosynthesis-active light. This information leads naturally to a series of materials - often used as coatings - for energy efficient glazings. We then focus on electrochromics, and Section III reports on a basic device design, a case study for the electrochromism in tungsten oxide, general considerations for the microstructure and electronic bands in electrochromic oxides, and some practical approaches to smart windows. Section IV gives a few final remarks.

II. AMBIENT RADIATION AND MATERIALS OPTIONS

A. Ambient Radiative Properties

The basic principles of materials for energy efficiency and solar energy conversion can be grasped only if one has a clear idea of the radiation that prevails in our natural surroundings.[1] This radiation is introduced in Fig. 1, where the different spectra are drawn with a common logarithmic wavelength scale. We start with the ideal blackbody, whose emitted spectrum is uniquely defined if the absolute temperature is known. Figure 1(a) depicts blackbody spectra for four temperatures. The vertical scale denotes power per unit area and wavelength increment. The spectra are confined to the $2 < \lambda < 100$ μm wavelength range. At room temperature the peak lies at about 10 μm. Thermal radiation from a real material is obtained by multiplying the blackbody spectrum by a wavelength-dependent factor - the emittance - which is less than unity.

Figure 2(b) reproduces a solar spectrum for radiation outside the earth's atmosphere. The curve is defined by the sun's surface temperature (~6000°C). The solar spectrum is limited to the $0.25 < \lambda < 3$ μm interval, so that there is almost no overlap with the spectra for thermal radiation. Hence one can have

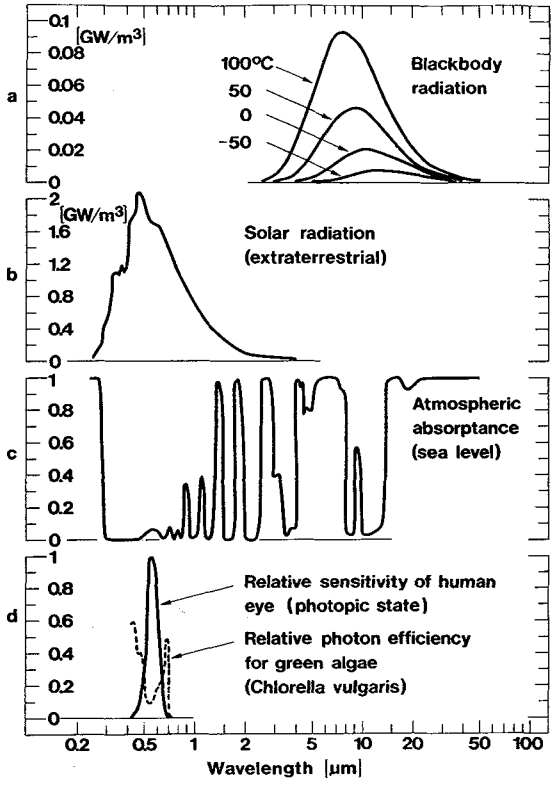

Fig. 1 Spectra for (a) blackbody radiation pertaining to four temperatures, (b) solar radiation outside the earth's atmosphere, (c) typical absorptance across the full atmospheric envelope, (d) relative sensitivity of the human eye and relative photon efficiency of green algae. (From Ref. 1).

materials whose properties are entirely different with regard to thermal and solar radiation. The integrated area under the curve gives the solar constant (1353±21 W m^{-2}); this is the largest possible power density on a surface oriented perpendicular to the sun in the absence of atmospheric extinction.

We are concerned with systems at ground level, and it is of obvious interest to consider to what extent atmospheric absorption influences solar irradiation and thermal emission. Figure 1(c) illustrates a typical absorption spectrum vertically across the full atmospheric envelope at clear weather conditions. The spectrum is complicated with bands of high absorption - caused mainly by water vapour, carbon dioxide, and ozone - and intervening bands of high transparency. The majority of the solar radiation can be transmitted down to ground level.

Thermal radiation from a surface exposed to the clear sky is strongly absorbed except in the $8 < \lambda < 13$ μm range, where the transmittance can be large provided that the humidity is moderately low. The thermal radiation can be large in the $8 < \lambda < 13$ μm interval, and hence a non-negligible part of the emitted energy can go straight through the atmosphere. This phenomenon constitutes the basis for radiative cooling.

Figure 1(d) illustrates two biophysical constraints of interest for glazings. The solid curve shows the relative spectral sensitivity of the human eye in its light-adapted (photopic) state. The bell-shaped curve extends across the $0.4 < \lambda < 0.7$ μm interval and has its peak at 0.555 μm. Clearly a large part of the solar energy comes as infrared radiation. Photosynthesis in plants operates with wavelengths in approximately the same range as those for the human eye, which is of relevance for greenhouses.

B. Survey of Coatings for Energy Efficient Glazings

Coatings can be used on glazings for obtaining several different goals. Table I summarizes these goals, gives the principle solutions, and lists the different types of materials used in the coatings.[2] In a warm

climate, the glazings normally let in too much energy, which must be balanced by air conditioning. The situation can be alleviated if the windows have coatings that are transparent primarily for visible light, i.e. at $0.4 < \lambda < 0.7$ μm, whereas they are reflecting for near-infrared solar radiation at $0.7 < \lambda < 3$ μm. A thin metal (Me) film can combine a transmittance of ~ 50 % in the visible range with a high infrared reflectance. However such a film is too absorbing for many applications, and instead the metal film could be put between two dielectric (D) layers which, in effect, antireflect the metal. A D/Me/D coating with Me = Ag can have ~ 80 % visible transmittance.

Table I. General properties of coatings for energy-efficient glazings

Goal	Principle solution	Coating material*
Diminished solar heating	Reflectance at $0.7 < \lambda < 3$ μm	Me or D/Me/D
	Angular dependent transmittance	D/Me/D/Me/D Oblique columnar metal
Thermal insulation	Reflectance at $3 < \lambda < 50$ μm	D/Me/D, SnO_2:F;In_2O_3:Sn, ZnO:Al...
Dynamic radiation control	Absorptance or reflectance in electrochromic material	Li_xWO_3, NiO_xH_y,... in multilayer design with transparent ion conductor
	Reflectance at $0.7 < \lambda < 3$ μm in thermochromic material	VO_2-based
Higher transmittance	Antireflectance at $\lambda \approx 0.55$ μm	AlO_xF_y,...

* Me is Ag, Cu, Au (or Al); D is Bi_2O_3, In_2O_3, SnO_2, TiO_2, ZnO or ZnS.

Another way to diminish the solar inflow is to exploit angular-selective window coatings.[3,4] The underlying idea is that windows are devices for creating visual contact with the outside world along an approximately horizontal line-of-sight, whereas solar radiation normally enters from a point much higher up on the vault of heaven. It follows that one can obtain energy efficiency by having coatings with high transmittance horizontally and a much lower transmittance at other angles. A properly tailored D/Me/D/Me/D coating can be useful for ordinary vertical windows. Angular selectivity can be created also for sloping glazings; in this case the coatings can be comprised of inclined columns produced by oblique angle vacuum deposition. For the latter case, one has a higher transmittance along the columns than across them, as one expects from theory.

In a cold climate, one normally wants to have glazings that combine a high solar transmittance at $0.3 < \lambda < 3$ μm with a high reflectance (i.e., a low emittance) for thermal radiation at $3 < \lambda < 50$ μm. D/Me/D coatings can be optimized for these wavelength intervals, but it may be more cost-effective to invoke films of certain heavily doped wide-bandgap oxide semiconductors such as In_2O_3:Sn, SnO_2:F, SnO_2:Sb and ZnO:Al. When the doping level is high enough, the semiconductors become strongly *n*-doped and can be reflecting at wavelenghts longer than a plasma wavelength that can be between 1 and 3 μm depending on the doping level and the degree of crystallinity.[5,6]

The heavily doped semiconductors are amenable to quantitative theoretical analysis.[5,6] Essentially, three components are added to form the complex dielectric function, viz. (i) the *contribution due to bound electrons* (accounting for bandgap widening due to the Burstein Moss effect partly balanced by electron-ion and electron-electron interaction[7,8]), (ii) the *contribution due to free electrons* undergoing

ionized impurity scattering against Coulomb-like potentials screened in accordance with the Random Phase Approximation or an extension thereof, and (iii) *phonon contributions* that can be modeled as a series of Lorentz oscillators. Figure 2 shows an example for the computed transmittance and reflectance of a 0.2-μm-thick film of In_2O_3:Sn doped so that the electron density n_e had the shown values.[5] Increasing the electron (or, equivalently, the dopant) density gives a material combining a high visible transmittance with a high thermal infrared reflectance.

A dynamic control of the optical properties is possible in smart windows with chromogenic coatings. The presently most viable alternatives are electrochromic films in multilayer devices, as discussed in the following section, and thermochromic films. Among the thermochromic films, the most important ones are based on VO_2. This material undergoes a transformation from a semiconducting and rather transparent state to a metallic and less transparent state when a temperature of ~ 68°C is exceeded. This phase change temperature can be diminished to room temperature by alloying with tungsten[9] and the transmittance can be boosted by fluorine incorporation.[10]

III. ELECTROCHROMICS AND SMART WINDOWS

A. Background

Electrochromic devices are able to change their optical properties in a reversible and persistent manner under the action of a voltage pulse. The optical modulation is related to the amount of mobile ions in an electrochromic material, which here is taken to be a metal oxide. The devices comprise several layers backed by a substrate (normally a glass plate) or layers positioned in between two substrates in a laminate configuration.[11] The substrate has a transparent conducting film and a film of the electrochromic oxide. Then follow a fast ion conductor or electrolyte, a layer serving as ion storage - which can be another electrochromic material - and a second (transparent) conductor. When a voltage is applied between the (transparent) conductors, ions are inserted into or extracted from the electrochromic film, whose optical properties thereby are changed. The design is outlined in Fig. 3. The insertion/extraction process can be represented, high schematically, by

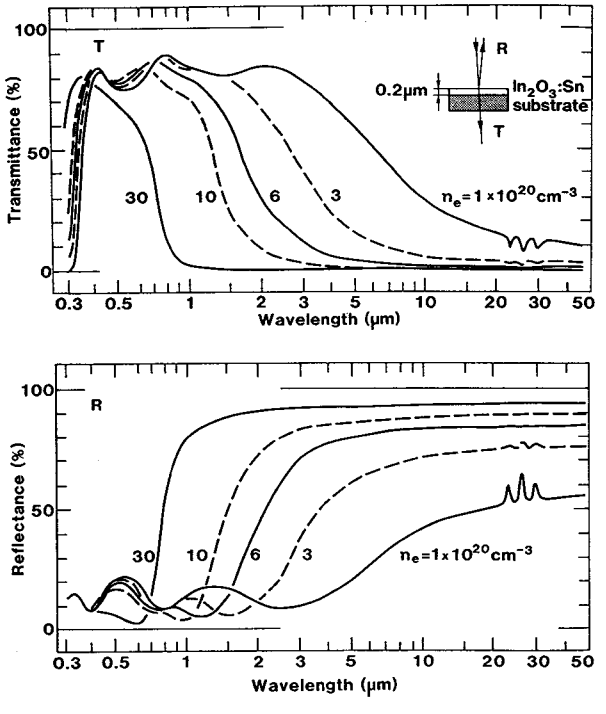

Fig. 2 Spectral normal transmittance (upper part) and reflectance (lower part) computed from a quantitative model for the optical properties of In_2O_3:Sn. The shown values of electron density (n_e) and thickness were used. (From Ref. 5).

$$MeO_y + xI^+ + xe^- \leftrightarrow I_xMeO_y, \quad (1)$$

where I^+ is a singly charged small ion such as H^+ or Li^+, e^- is an electron, and y depends on the particular type of oxide. For example, y is 3 for defect perovskites and 2 for rutiles.

Electrochromic devices have several important applications that presently spur the scientific and technical development. Foremost among these are smart windows capable of regulating the inflow of radiant energy through glazings so that an optimum indoor climate is maintained at a minimum demand on paid energy.

B. Electrochromism in W Oxide: A Case Study (Ref. 11)

Electrochromism was discovered in W oxide films, and this material remains still today the most promising with regard to practical applications. There are many techniques for making W oxide films. Evaporation, sputtering and a number of chemical and electrochemical methods all are applicable and are able to produce non-stoichiometric WO_3 films with a porosity of up to 50 %. Raman scattering and X-ray extinction, in particular, have been used to formulate structural models[12] showing that the films are built, from clusters of corner-sharing octahedra.

W oxide films have been studied extensively in liquid electrolytes by use of the conventional techniques of electrochemistry. Coulometric titration, chronoamperometry, cyclic voltammetry, impedance spectrometry, beam deflectometry, and microbalance techniques[11] have been applied. The diffusion constants for intercalation/deintercalation of H^+ and Li^+ lie in the ranges 10^{-10} to 2.5×10^{-7} and 1.5×10^{-12} to 5×10^{-9} cm^2/s, respectively.

X-ray photoelectron spectroscopy in the energy range pertinent to W4f electrons show peaks that allow the amount of W atoms in different valence states to be calculated. For H_xWO_3 with $x = 0.09$ it was possible to represent the spectrum with two sets of peaks assigned to W^{5+} and W^{6+}, and at $x = 0.42$ there was clear evidence also for W^{4+}.[13] Electron paramagnetic resonance is capable of providing additional information on the valence state of the W ion since W^{5+} ($5d^1$ configuration) gives a signal due to its unpaired spin whereas W^{6+} ($5d^0$ configuration) does not. Experimental data showed unambiguously that a signal assigned to W^{5+} developed upon H^+ intercalation.[14]

Figure 4 shows the modulation of the spectral transmittance upon intercalation to the shown charge densities in a H^+-conducting electrolyte.[16] The W-oxide-based film can change reversibly and gradually from a virtually transparent state to a state characterized by a low transmittance of blue light.

C. Microstructure and Electronic Bands: A Unified Approach (Ref. 17)

The electrochromic oxides can be divided into three main groups with regard to their bulk crystalline structures: perovskite-like, rutile-like, and layer and block structures. They are discussed in this order

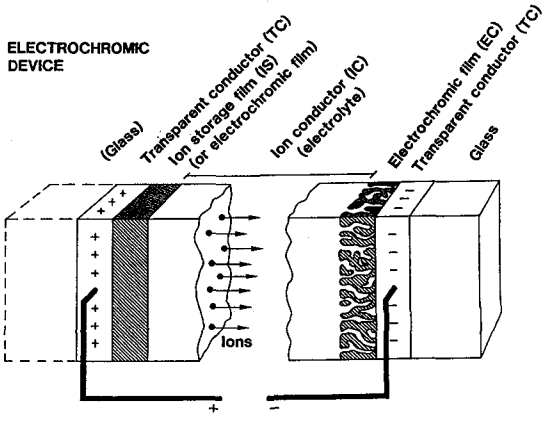

Fig. 3 Basic design of an electrochromic device, indicating transport of positive ions under the action of an electric field.

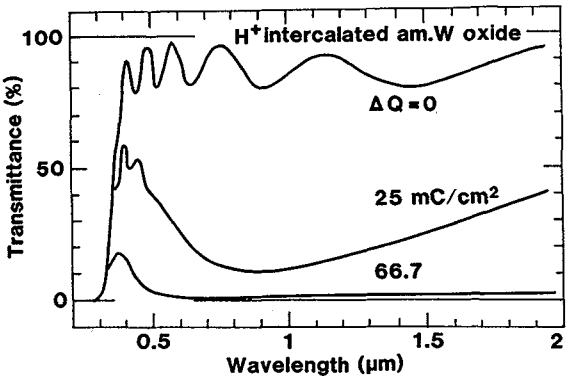

Fig. 4 Spectral transmittance for an amorphous (am.) W oxide film with H+ intercalation to the shown charge densities. (From Ref. 16).

below, and the ubiquity of the octahedral MeO_6 building blocks is emphasized. Reference 18 may serve as a standard source for much of the structural information. Along with the discussion of structure, we point at characteristic features of the electrochromism.

The *perovskite structure,* with a general composition $CMeO_3$, is illustrated in Fig. 5. The Me ions occupy the corners of a primitive unit cell and O ions bisect the unit cell edges. The central atom, denoted C, is absent in the electrochromic oxides of most interest. The corresponding (defect) perovskite MeO_3 configuration can be visualized as an infinite array of corner-sharing octahedra each with a metal ion surrounded by six equidistant oxygen ions. In between these octahedra there are extended tunnels that can serve as conduits and intercalation sites for small ions.

Tungsten oxide, WO_3, has a crystal structure of perovskite-type; it has a tendency to form substoichiometric (Magnéli) phases with edge-sharing octahedra and extended tunnels with large pentagonal or hexagonal cross-sections. As discussed above, disordered W oxide films transform from an optically transparent to an absorbing state under ion insertion. This is referred to, in electrochemical terms, as *cathodic colouration.* The opposite case, with absorption associated with ion extraction, is called *anodic colouration.* Molybdenum oxide, MoO_3, is another cathodic electrochromic material. Available data on thin films strongly indicate that the structure is built from corner-sharing MoO_6 octahedra in much the same way as for electrochromic W oxide.

The *rutile structure,* or at least a rutile-like configuration, is present for a whole series of materials exhibiting cathodic or anodic electrochromism. The ideal structure can be thought of as built from almost octahedral MeO_6 units forming infinite edge-shared chains. These chains are arranged so that they form an equal number of ideal vacant tunnels.

Titanium oxide, TiO_2, can have different crystal structures; the anatase phase has so far attracted most interest, and cathodic electrochromism with a large degree of optical modulation has been observed. Manganese oxide, MnO_2, has very complex crystal chemistry. However, most structures are built from edge-shared MnO_6 octahedra. Electrochromism was discovered recently, and ion insertion was found to lower the absorption. Vanadium dioxide, VO_2, is of rutile-type (tetragonal) above 68°C and is monoclinic below this temperature. Vanadium dioxide films are electrochromic and show a decrease of the absorptance under ion insertion irrespective of temperature. Ruthenium oxide, RuO_2, has a rutile structure. Ions can be inserted and extracted, but the material remains absorbing no matter the ionic content. Iridium oxide, IrO_2, is another rutile material. It is electrochromic and - in contrast with the electrochromic oxides discussed so far - is clearly anodic and can go from an absorbing to a fully transparent state under insertion of one ion per formula unit. Rhodium oxide, RhO_2, shows many similarities with iridium oxide, and ion insertion is able to lower the absorption significantly.

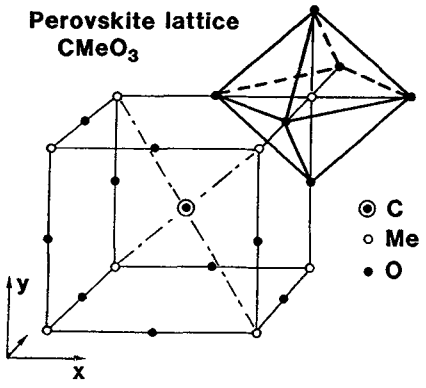

Fig. 5 Unit cell for the perovskite lattice. Octahedral symmetries are emphasized.

The *layer and block structures* are considered next. Hydrous Ni oxide shows pronounced anodic electrochromism and goes from an absorbing to a transparent state under proton insertion. The material contains layers of NiO_6 octahedra sharing edges, and the protonated material is probably akin to brucite, $Ni(OH)_2$. Vanadium pentoxide, V_2O_5, can be described as consisting of distorted VO_6 octahedra or, alternatively and perhaps more properly, as consisting of square pyramidal VO_5 units. The latter representation highlights the layered structure. V pentoxide films have a capacity for multicolour electrochromism. Niobium oxide, Nb_2O_5, has complex crystal chemistry but most phases are built from blocks (or columns) of NbO_6 octahedra arranged as in a defect perovskite.

The structural similarities of the electrochromic materials make it meaningful to discuss their optical properties from a canonical bandstructure appropriate to the octahedral coordination. These highly simplified bandstructures, originally due to Goodenough[19] and presented in a particularly accessible way by Honig,[20] allow us to understand why certain perovskite-type and rutile-type electrochromic oxides become absorbing under ion insertion, others become transparent under ion insertion, and still others show at least some absorptance irrespective of their ionic content.

The *perovskite structure* was illustrated in Fig. 5. A corresponding energy level diagram for the defect perovskite is illustrated in Fig. 6a. The atomic *s*, *p* and *d* levels of Me are indicated, as well as the *2s* and *2p* levels of O. As a consequence of the octahedral coordination, the *d* level is split into e_g and t_{2g} levels. Similarly,there is a splitting into $O2p_\sigma$ and $O2p_\pi$. The incipient molecular energy levels broaden into bands, whose relative widths and repulsion can be inferred from general arguments.[20]

The number of states available for electron occupancy is fixed for each band. Counted per MeO_3 formula unit, the t_{2g} band has a capacity for six electrons and the p_π band has a capacity for twelve electrons. WO_3 and the iso-structural β-MoO_3 have 24 electrons in the shown bands, so that the Fermi energy lies in the gap between the t_{2g} and p_π bands. The bandgap is wide enough to render the material transparent.

When ions and electrons are inserted according to reaction (1), the Fermi level is moved upwards in the presumed rigid-band scheme. In the case of WO_3 and β-MoO_3, the excess electrons must enter the t_{2g} band and the material, in principle, transforms from a transparent to an absorbing or from a transparent to a reflecting state depending on whether the electrons occupy localized or extended states. When the ions and the accompanying electrons are extracted, the material returns to its original transparent state.

The *rutile structure* leads to the schematic bandstructure illustrated in Fig. 6b. It deviates somewhat from its counterpart for the perovskites because the MeO_6 building blocks are distorted and edge-sharing. The arrows in the left-hand part of Fig. 6b indicate the Fermi levels for several oxides. For TiO_2, the Fermi level lies in the gap between the $Ti3t_{2g}$ and the $O2p_\perp$ bands, and ion insertion is expected to lead to a transformation from a transparent to an absorbing state. This is consistent with experimental results. For VO_2, MnO_2 and RuO_2, the initial absorbing state can not be eliminated by ion insertion. Again this is as expected from the bandstructure. RhO_2 and IrO_2 are especially interesting, since their Fermi levels lie

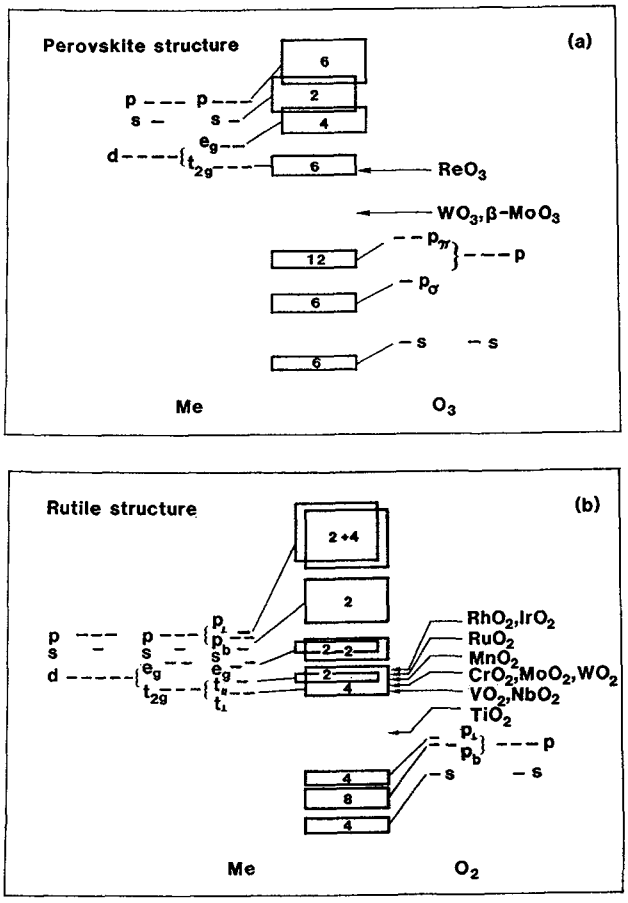

Fig. 6 Schematic bandstructures for the MeO_3 defect perovskite structure (a) and the MeO_2 rutile structure (b). The incipient atomic and molecular levels are shown, using standard notation. The numbers in the different bands denote electron capacities. Arrows indicate Fermi energies. (From Ref. 20).

close to the gap between the t_{2g} and e_g bands. Indeed, if ions are inserted up to about one formula unit in an Ir oxide film, it is transformed from an absorbing to a transparent state. In the bandstructure picture, the transparency is associated with the bandgap referred to above. Rhodium oxide films are similar to Ir oxide films.

D. Towards the Electrochromic Smart Window (Refs. 11, 21)

Practical electrochromic devices have an electrolyte at their center as seen in Fig. 3. Liquid electrolytes, that are commonly used in laboratory studies, are not of interest for practical window applications. Also many of the standard members of the solid state ionics zoo (β-aluminas, Nasicons, etc.) are not easily used since it is difficult to make thin films of them. Hydrated oxide films are of relevance, and devices with a Ta_2O_5:H_2O film in between layers of cathodic electochromic W oxide and anodic electrochromic Ni oxide are currently exploited for rear-view mirrors in automobiles. Whereas this approach may be suitable for small devices, one may question its usefulness in large smart windows to be used for energy-efficient glazings. It appears that polymer electrolytes are more promising for smart windows.

Extensive work has been carried out with proton conducting polymers such as polysulfonic acids. These polymers tend to corrode W oxide films, though, and therefore the interest has shifted more towards Li+ conducting polymers. Initial work was reported for devices with polyethylene oxide (PEO) incorporating $LiClO_4$.[22] These "windows" exhibit temperature dependent electrochromism, but operation at room

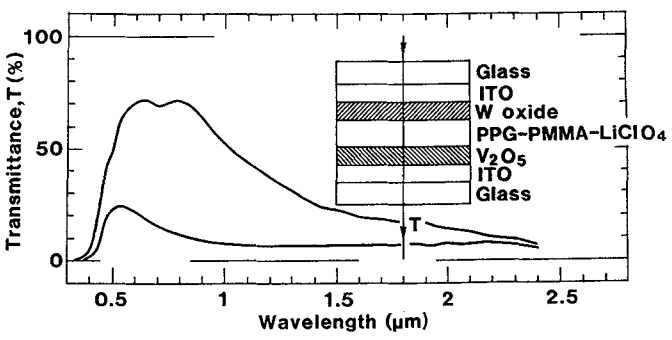

Fig. 7 Spectral transmittance in coloured and bleached states for an electrochromic device with a Li+-conducting electrolyte. The design is sketched in the inset. (From Ref. 24).

temperature requires more conducting electrolytes. One interesting possibility is PEO-$LiN(SO_2CF_3)_2$, which was used in some recent studies.[23] Devices with amorphous W oxide and ion storage layers of V_2O_5 showed transmittance modulation between ~41 and ~13 % at $\lambda = 0.633$ μm. Device operation at room temperature is possible also with multilayer structures based on W oxide, V_2O_5, and an intervening adhesive electrolyte of poly propylene glycol (PPG) and poly methyl methacrylate (PMMA).[24] Figure 7 illustrates the latter design and shows spectral transmittance in coloured and bleached states. At $\lambda = 0.633$ μm, for example, the transmittance can be modulated between as much as ~72 and ~20 %. Results are available also with lithiated Ni oxide used as ion storage layer.

IV CONCLUDING REMARKS

A large number of novel materials can be used for solar energy applications and for creating energy efficiency in many different contexts. Some of these materials are now reaching maturation, such as selectively solar-absorbing films and transparent infrared-reflecting films for architectural glazings. Other materials still have a way to go before they can reach commercialization; smart windows based on electrochromism and thermochromism belong to this class. Large area chromogenics, electrochromism, and smart windows are likely to have important applications in benign buildings technology. Electrochromism has been known for some 25 years but has so far eluded a fundamental theoretical approach. This paper summarized some recent advances in our understanding of the basic microstructures of the relevant oxides and of their ensuing electronic bands.

REFERENCES

[1] GRANQVIST C.G., editor, Materials Science for Solar Energy Conversion Systems (Pergamon, Oxford, 1991).
[2] GRANQVIST C.G., in Ref. 1, p. 106.
[3] MBISE G., SMITH G.B., NIKLASSON G.A. and GRANQVIST C.G., *Appl. Phys. Lett.* **54** (1989) 987.
[4] SMITH G.B., NG M.W., DITCHBURN R.J., MARTIN P.J. and NETTERFIELD R.P., *Solar Energy Mater. Solar Cells* **25** (1992) 149.
[5] HAMBERG I. and GRANQVIST C.G., *J. Appl. Phys.* **60** (1986) R123.
[6] JIN Z.-C., HAMBERG I. and GRANQVIST C.G., *J. Appl. Phys.* **64** (1988) 5117.
[7] HAMBERG I., GRANQVIST C.G., BERGGREN K.-F., SERNELIUS B.E. and ENGSTRÖM L., *Phys. Rev. B* **30** (1984) 3240.
[8] SERNELIUS B.E., BERGGREN K.-F., JIN Z.-C., HAMBERG I. and GRANQVIST C.G., *Phys. Rev. B* **37** (1988) 10244.
[9] SOBHAN A. and GRANQVIST C.G., to be published.
[10] KHAN K.A. and GRANQVIST C.G., *Appl. Phys. Lett.* **55** (1989) 4.

[11] GRANQVIST C.G., in Physics of Thin Films, edited by M. Francombe and J. Vossen (Academic, San Diego, 1993), Vol. 17, to be published.
[12] NANBA T. and YASUI I., *J. Solid State Chem.* **83** (1989) 304.
[13] TEMMINK A., ANDERSON O., BANGE K., HANTSCHE H. and YU X., *Thin Solid Films* **192** (1990) 211.
[14] GÉRARD P., DENEUVILLE A. and COURTHS R., *Thin Solid Films* **71** (1980) 221.
[15] SCHIRMER O.F., WITTWER W., BAUR G. and BRANDT G., *J. Electrochem. Soc.* **124** (1977) 749.
[16] MIYAKE K., KANEKO H., SANO M. and SUEDOMI N., *J. Appl. Phys.* **55** (1984) 2747.
[17] GRANQVIST C.G., *J. Mater. Sci. Engr.*, to be published; *Z. Phys.* B, to be published.
[18] HYDE B.G. and ANDERSSON S., Inorganic Crystal Structures (Wiley, New York, 1989).
[19] GOODENOUGH J.B., in Progress in Solid State Chemistry, edited by H. Reiss (Pergamon, Oxford, 1971), Vol. 5, p. 145.
[20] HONIG J.M., in Electrodes of Conductive Metallic Oxides, Part A, edited by S. Trasatti (Elsevier, Amsterdam, 1980), p. 1.
[21] GRANQVIST C.G., *Solid State Ionics* **53-56** (1992) 479.
[22] PANTALONI S., PASSERINI S. and SCROSATI B., *J. Electrochem. Soc.* **134** (1987) 753.
[23] BAUDRY P., AEGERTER M.A., DEROO D. and VALLA B., *J. Electrochem. Soc.* **138** (1991) 460.
[24] ANDERSSON A.M., GRANQVIST C.G. and STEVENS J.R., *Appl. Opt.* **28** (1989) 3295.